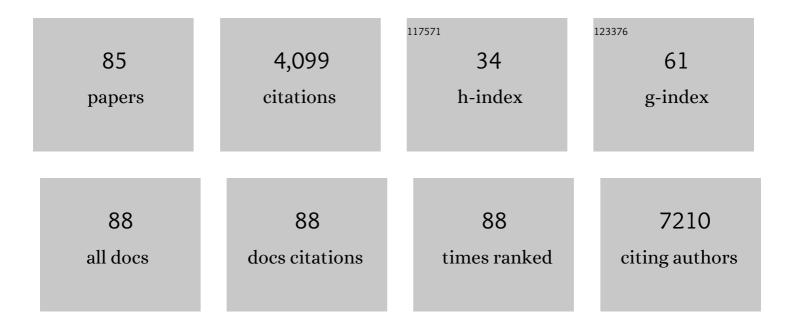
List of Publications by Year in descending order

Source: https://exaly.com/author-pdf/4228580/publications.pdf Version: 2024-02-01



#	Article	IF	CITATIONS
1	3d transition metal coordination on monolayer MoS <sub>2</sub> : a facile doping method to functionalize surfaces. Nanoscale, 2022, 14, 10801-10815.	2.8	5
2	Confined Crack Propagation in MoS <sub>2</sub> Monolayers by Creating Atomic Vacancies. ACS Nano, 2021, 15, 1210-1216.	7.3	19
3	Photodegradation Protection in 2D In-Plane Heterostructures Revealed by Hyperspectral Nanoimaging: The Role of Nanointerface 2D Alloys. ACS Nano, 2021, 15, 2447-2457.	7.3	14
4	Growth manner of rod-shaped ZnO crystals at low temperature without any seed/buffer layer on a polyimide film. CrystEngComm, 2021, 23, 2039-2047.	1.3	1
5	Quantification and Healing of Defects in Atomically Thin Molybdenum Disulfide: Beyond the Controlled Creation of Atomic Defects. ACS Nano, 2021, 15, 9658-9669.	7.3	37
6	Multiple excitations and temperature study of the disorder-induced Raman bands in MoS <sub>2</sub> . 2D Materials, 2021, 8, 035042.	2.0	6
7	Defect creation in WSe <sub>2</sub> with a microsecond photoluminescence lifetime by focused ion beam irradiation. Nanoscale, 2020, 12, 2047-2056.	2.8	30
8	Controlled Fragmentation of Single-Atom-Thick Polycrystalline Graphene. Matter, 2020, 2, 666-679.	5.0	45
9	Nonlinear Dark-Field Imaging of One-Dimensional Defects in Monolayer Dichalcogenides. Nano Letters, 2020, 20, 284-291.	4.5	34
10	Second harmonic generation in two-dimensional transition metal dichalcogenides with growth and post-synthesis defects. 2D Materials, 2020, 7, 045020.	2.0	10
11	Monolayer Vanadiumâ€Doped Tungsten Disulfide: A Roomâ€Temperature Dilute Magnetic Semiconductor. Advanced Science, 2020, 7, 2001174.	5.6	104
12	Spontaneous chemical functionalization via coordination of Au single atoms on monolayer MoS <sub>2</sub> . Science Advances, 2020, 6, .	4.7	56
13	Single-atom doping of MoS <sub>2</sub> with manganese enables ultrasensitive detection of dopamine: Experimental and computational approach. Science Advances, 2020, 6, eabc4250.	4.7	136
14	Superconductivity enhancement in phase-engineered molybdenum carbide/disulfide vertical heterostructures. Proceedings of the National Academy of Sciences of the United States of America, 2020, 117, 19685-19693.	3.3	6
15	Electric field induced metallic behavior in thin crystals of ferroelectric <b> <i>α</i> </b> -In2Se3. Applied Physics Letters, 2020, 117, .	1.5	17
16	Universal <i>In Situ</i> Substitutional Doping of Transition Metal Dichalcogenides by Liquid-Phase Precursor-Assisted Synthesis. ACS Nano, 2020, 14, 4326-4335.	7.3	100
17	Interface-mediated noble metal deposition on transition metal dichalcogenide nanostructures. Nature Chemistry, 2020, 12, 284-293.	6.6	73
18	PbS-quantum-dots/double-wall-carbon-nanotubes nanohybrid based photodetectors with extremely fast response and high responsivity. Materials Today Energy, 2020, 16, 100378.	2.5	12

#	Article	IF	CITATIONS
19	Hybridized double-walled carbon nanotubes and activated carbon as free-standing electrode for flexible supercapacitor applications. Carbon Letters, 2020, 30, 527-534.	3.3	20
20	Functional hetero-interfaces in atomically thin materials. Materials Today, 2020, 37, 74-92.	8.3	21
21	Surfactant-Mediated Growth and Patterning of Atomically Thin Transition Metal Dichalcogenides. ACS Nano, 2020, 14, 6570-6581.	7.3	30
22	Outer Tube-Selectively Boron-Doped Double-Walled Carbon Nanotubes for Thermoelectric Applications. ACS Applied Nano Materials, 2020, 3, 3347-3354.	2.4	8
23	Clean Transfer of 2D Transition Metal Dichalcogenides Using Cellulose Acetate for Atomic Resolution Characterizations. ACS Applied Nano Materials, 2019, 2, 5320-5328.	2.4	33
24	Dynamics of cleaning, passivating and doping monolayer MoS <sub>2</sub> by controlled laser irradiation. 2D Materials, 2019, 6, 045031.	2.0	40
25	Synthesis of V-MoS <sub>2</sub> Layered Alloys as Stable Li-Ion Battery Anodes. ACS Applied Energy Materials, 2019, 2, 8625-8632.	2.5	19
26	Carbon doping of WS <sub>2</sub> monolayers: Bandgap reduction and p-type doping transport. Science Advances, 2019, 5, eaav5003.	4.7	119
27	Electrochemically Exfoliated Graphene Electrode for High-Performance Rechargeable Chloroaluminate and Dual-Ion Batteries. ACS Applied Materials & Interfaces, 2019, 11, 23261-23270.	4.0	40
28	Controlling Nitrogen Doping in Graphene with Atomic Precision: Synthesis and Characterization. Nanomaterials, 2019, 9, 425.	1.9	67
29	Defect-mediated selective hydrogenation of nitroarenes on nanostructured WS <sub>2</sub> . Chemical Science, 2019, 10, 10310-10317.	3.7	30
30	Structural and electrochemical properties of babassu coconut mesocarp-generated activated carbon and few-layer graphene. Carbon, 2019, 145, 175-186.	5.4	52
31	Facile 1D graphene fiber synthesis from an agricultural by-product: A silicon-mediated graphenization route. Carbon, 2019, 142, 78-88.	5.4	14
32	Angstrom-Size Defect Creation and Ionic Transport through Pores in Single-Layer MoS <sub>2</sub> . Nano Letters, 2018, 18, 1651-1659.	4.5	129
33	Pyrolytic carbon supported alloying metal dichalcogenides as free-standing electrodes for efficient hydrogen evolution. Carbon, 2018, 132, 512-519.	5.4	18
34	Lightâ€Emitting Transition Metal Dichalcogenide Monolayers under Cellular Digestion. Advanced Materials, 2018, 30, 1703321.	11.1	13
35	Carbon-rich shungite as a natural resource for efficient Li-ion battery electrodes. Carbon, 2018, 130, 105-111.	5.4	31
36	Raman spectroscopy revealing noble gas adsorption on single-walled carbon nanotube bundles. Carbon, 2018, 127, 312-319.	5.4	26

#	Article	IF	CITATIONS
37	Electrochemical Exfoliation: On the Role of Transition Metal Salts During Electrochemical Exfoliation of Graphite: Antioxidants or Metal Oxide Decorators for Energy Storage Applications (Adv. Funct. Mater. 48/2018). Advanced Functional Materials, 2018, 28, 1870345.	7.8	0
38	On the Role of Transition Metal Salts During Electrochemical Exfoliation of Graphite: Antioxidants or Metal Oxide Decorators for Energy Storage Applications. Advanced Functional Materials, 2018, 28, 1804357.	7.8	32
39	Probing the interaction of noble gases with pristine and nitrogen-doped graphene through Raman spectroscopy. Physical Review B, 2018, 97, .	1.1	7
40	Nanostructured carbon materials for enhanced nitrobenzene adsorption: Physical vs. chemical surface properties. Carbon, 2018, 139, 833-844.	5.4	55
41	H2O2/UV layer-by-layer oxidation of multiwall carbon nanotubes: The "onion effect―and the control of the degree of surface crystallinity and diameter. Carbon, 2018, 139, 1027-1034.	5.4	10
42	CO2 Sensing by in-situ Raman spectroscopy using activated carbon generated from mesocarp of babassu coconut. Vibrational Spectroscopy, 2018, 98, 111-118.	1.2	31
43	Effect of boron doping on the electrical conductivity of metallicity-separated single walled carbon nanotubes. Nanoscale, 2018, 10, 12723-12733.	2.8	37
44	Excitonic processes in atomically-thin MoSe <sub>2</sub> /MoS <sub>2</sub> vertical heterostructures. 2D Materials, 2018, 5, 031016.	2.0	12
45	Monolayer WS <sub>2</sub> Nanopores for DNA Translocation with Light-Adjustable Sizes. ACS Nano, 2017, 11, 1937-1945.	7.3	102
46	Low-temperature Synthesis of Heterostructures of Transition Metal Dichalcogenide Alloys (W <sub><i>x</i></sub> Mo <sub>1–<i>x</i></sub> S <sub>2</sub> ) and Graphene with Superior Catalytic Performance for Hydrogen Evolution. ACS Nano, 2017, 11, 5103-5112.	7.3	157
47	Photoluminescence Segmentation within Individual Hexagonal Monolayer Tungsten Disulfide Domains Grown by Chemical Vapor Deposition. ACS Applied Materials & Interfaces, 2017, 9, 15005-15014.	4.0	59
48	Optical identification of sulfur vacancies: Bound excitons at the edges of monolayer tungsten disulfide. Science Advances, 2017, 3, e1602813.	4.7	213
49	Solution synthesis of few-layer WTe <sub>2</sub> and Mo <sub>x</sub> W <sub>1â^²x</sub> Te <sub>2</sub> nanostructures. Journal of Materials Chemistry C, 2017, 5, 11317-11323.	2.7	23
50	Homogeneously dispersed CeO2 nanoparticles on exfoliated hexaniobate nanosheets. Journal of Physics and Chemistry of Solids, 2017, 111, 335-342.	1.9	11
51	Low-Temperature Solution Synthesis of Transition Metal Dichalcogenide Alloys with Tunable Optical Properties. Journal of the American Chemical Society, 2017, 139, 11096-11105.	6.6	68
52	Ordered and Atomically Perfect Fragmentation of Layered Transition Metal Dichalcogenides <i>via</i> Mechanical Instabilities. ACS Nano, 2017, 11, 9191-9199.	7.3	53
53	Intricate Resonant Raman Response in Anisotropic ReS <sub>2</sub> . Nano Letters, 2017, 17, 5897-5907.	4.5	66
54	Nobleâ€Metalâ€Free Hybrid Membranes for Highly Efficient Hydrogen Evolution. Advanced Materials, 2017, 29, 1603617.	11.1	73

#	Article	IF	CITATIONS
55	Photoluminescence Enhancement of Titanate Nanotubes by Insertion of Rare Earth Ions in Their Interlayer Spaces. Journal of Nanomaterials, 2017, 2017, 1-9.	1.5	19
56	A Review of Double-Walled and Triple-Walled Carbon Nanotube Synthesis and Applications. Applied Sciences (Switzerland), 2016, 6, 109.	1.3	44
57	Linear carbon chains inside multi-walled carbon nanotubes: Growth mechanism, thermal stability and electrical properties. Carbon, 2016, 107, 217-224.	5.4	33
58	Lowâ€Temperature Solution Synthesis of Few‣ayer 1T ′â€MoTe <sub>2</sub> Nanostructures Exhibitir Lattice Compression. Angewandte Chemie - International Edition, 2016, 55, 2830-2834.	<sup>1g</sup> 7.2	84
59	Distinct photoluminescence and Raman spectroscopy signatures for identifying highly crystalline WS <sub>2</sub> monolayers produced by different growth methods. Journal of Materials Research, 2016, 31, 931-944.	1.2	95
60	Multiple exciton generation induced enhancement of the photoresponse of pulsed-laser-ablation synthesized single-wall-carbon-nanotube/PbS-quantum-dots nanohybrids. Scientific Reports, 2016, 6, 20083.	1.6	23
61	Ultrasensitive molecular sensor using N-doped graphene through enhanced Raman scattering. Science Advances, 2016, 2, e1600322.	4.7	174
62	Lowâ€Temperature Solution Synthesis of Few‣ayer 1T ′â€MoTe 2 Nanostructures Exhibiting Lattice Compression. Angewandte Chemie, 2016, 128, 2880-2884.	1.6	22
63	High electrical conductivity of double-walled carbon nanotube fibers by hydrogen peroxide treatments. Journal of Materials Chemistry A, 2016, 4, 74-82.	5.2	41
64	Elucidating the local interfacial structure of highly photoresponsive carbon nanotubes/PbS-QDs based nanohybrids grown by pulsed laser deposition. Carbon, 2016, 96, 145-152.	5.4	15
65	Study of the growth of CeO2 nanoparticles onto titanate nanotubes. Journal of Physics and Chemistry of Solids, 2015, 87, 213-220.	1.9	31
66	Ultrasensitive gas detection of large-area boron-doped graphene. Proceedings of the National Academy of Sciences of the United States of America, 2015, 112, 14527-14532.	3.3	177
67	Graphene: Large-Area Si-Doped Graphene: Controllable Synthesis and Enhanced Molecular Sensing (Adv. Mater. 45/2014). Advanced Materials, 2014, 26, 7676-7676.	11.1	0
68	Facile synthesis of MoS2 and MoxW1-xS2 triangular monolayers. APL Materials, 2014, 2, .	2.2	93
69	Importance of open, heteroatom-decorated edges in chemically doped-graphene for supercapacitor applications. Journal of Materials Chemistry A, 2014, 2, 9532-9540.	5.2	91
70	Largeâ€Area Siâ€Doped Graphene: Controllable Synthesis and Enhanced Molecular Sensing. Advanced Materials, 2014, 26, 7593-7599.	11.1	116
71	Defect-Assisted Heavily and Substitutionally Boron-Doped Thin Multiwalled Carbon Nanotubes Using High-Temperature Thermal Diffusion. Journal of Physical Chemistry C, 2014, 118, 4454-4459.	1.5	17
72	Mechanically Tough, Electrically Conductive Polyethylene Oxide Nanofiber Web Incorporating DNA-Wrapped Double-Walled Carbon Nanotubes. ACS Applied Materials & Interfaces, 2013, 5, 4150-4154.	4.0	20

#	Article	IF	CITATIONS
73	A reversible strain-induced electrical conductivity in cup-stacked carbon nanotubes. Nanoscale, 2013, 5, 10212.	2.8	12
74	Boron-assisted coalescence of parallel multi-walled carbon nanotubes. RSC Advances, 2013, 3, 26266.	1.7	5
75	Formation of Nitrogen-Doped Graphene Nanoribbons <i>via</i> Chemical Unzipping. ACS Nano, 2013, 7, 2192-2204.	7.3	80
76	Controlled interlayer spacing of scrolled reduced graphene nanotubes by thermal annealing. RSC Advances, 2013, 3, 4161.	1.7	13
77	Multiple intra-tube junctions in the inner tube of peapod-derived double walled carbon nanotubes: theoretical study and experimental evidence. Nanoscale, 2012, 4, 130-136.	2.8	16
78	Raman Spectroscopy of Boron-Doped Single-Layer Graphene. ACS Nano, 2012, 6, 6293-6300.	7.3	245
79	Clean Nanotube Unzipping by Abrupt Thermal Expansion of Molecular Nitrogen: Graphene Nanoribbons with Atomically Smooth Edges. ACS Nano, 2012, 6, 2261-2272.	7.3	54
80	Determination of the stacking order of curved few-layered graphene systems. Nanoscale, 2012, 4, 6419.	2.8	5
81	Unusually High Dispersion of Nitrogen-Doped Carbon Nanotubes in DNA Solution. Journal of Physical Chemistry B, 2011, 115, 14295-14300.	1.2	8
82	Enhanced electrical conductivities of N-doped carbon nanotubes by controlled heat treatment. Nanoscale, 2011, 3, 4359.	2.8	60
83	Chirality-Dependent Transport in Double-Walled Carbon Nanotube Assemblies: The Role of Inner Tubes. ACS Nano, 2011, 5, 7547-7554.	7.3	28
84	Optically and Biologically Active Mussel Protein oated Doubleâ€Walled Carbon Nanotubes. Small, 2011, 7, 3292-3297.	5.2	31
85	Boron Atoms as Loop Accelerator and Surface Stabilizer in Plateletâ€Type Carbon Nanofibers. ChemPhysChem, 2010, 11, 2345-2348.	1.0	15